Three-Dimensional Light Manipulation by Gold Nanobumps

Chia Min Chang[a,b,d], Ming Lun Tseng[b,c], Bo Han Cheng[d,e], Cheng Hung Chu[b], You Zhe Ho[b], Hsin Wei Huang[b], Hung-Kuei Tsai[b], Kuang Sheng Chung[b], I-Da Chiang[b], Yueh-Hung Cheng[b], Yung-Chiang Lan[e], Ding-Wei Huang[a], Ai Qun Liu[f], Din Ping Tsai[b,c,d]*

[a]Graduate Institute of Photonics and Optoelectronics, National Taiwan University, Taipei 10617, Taiwan; [b]Department of Physics, National Taiwan University, Taipei 10617, Taiwan; [c]Graduate Institute of Applied Physics, National Taiwan University, Taipei 10617, Taiwan; [d]Research Center for Applied Sciences, Academia Sinica, Taipei 11529, Taiwan; [e]Department of Photonics, National Cheng Kung University, Tainan 701, Taiwan; [f]School of Electrical and Electronic Engineering, Nanyang Technological University, Singapore

ABSTRACT

The scattering of surface plasmon polariton (SPP) waves can be manipulated by various plasmonic structures. The plasmonic structure composed of arranged subwavelength nanobumps on a gold thin film is the promising structure to manipulation SPP wave. By controlling the geometric shape of the structures, the height, position, and pattern of scattered light from SPP wave can be modulated as desired. A clear single focusing spot can be reconstructed at a specific altitude by a particular curved structure with appropriate curvature and adjacent interspacing of nanobumps. The designed light patterns reconstructed by the focusing spot from the arranged curved structures at a specific observation plane are clearly demonstrated.

Keywords: Plasmonic projection; Light manipulation; Surface plasmon; Scattering; Focusing

1. INTRODUCTION

Surface plasmon polaritons (SPP), known as electromagnetic surface wave propagating at the interface between a dielectric and conductor, have been found great application potential in numerous field[1], such as nanoscale optical devices[2-3], solar cell[4], plasmonic laser[5], sensing[6-7], super lens[8-9], metamaterials, and cancer cell treatment[10]. In widely application fields, how to control and manipulate the light by using plasmonic nanostructure is one of critical research issues of plasmonics. Using quarter circular structure to focusing and guiding surface plasmon wave is firstly demonstrated the subwavelength focusing breaking the diffraction limit of conventional optics.[11] Theoretical calculation and experiments are both demonstrated the surface plasmon wave guiding and focusing achieved by chains of nanoparticles on thin metallic films.[12] Even various kinds of optical devices, such as SPP mirror, beam splitter and interferometer, are developed in two-dimensional optics.[13] However, it can be noted that most of reports on the manipulation of surface plasmon wave are remaining in the same plane. In fact, the behaviors of surface plasmon wave interacted with nanostructure are not only the in-plane scattering, namely near-field reflection and transmission, but also the out of plane scattering, that is far-field propagated light.[14] Converting the surface plasmon wave to propagated wave that radiate to the far field is theoretically proposed by several ways, such as a plasmonic chain resonator,[15] structured grating.[16] The theoretical simulation of structured grating proposed by a strict design method is reported the efficient far field scattering conversion, that can theoretically achieve out of plane focusing at several wavelengths away from surface. Therefore, it opens the possibility for three dimensional integrated photonic circuits application by way of using a nanostructure to control the far-field scattering of surface plasmon wave.

In our previous research,[17] the out of surface focusing and diverging of surface plasmon wave scattered by quarter circular structure composed of gold (Au) nanobumps is clearly demonstrated. Three dimensional propagation wave vectors for backward and forward scattering light are generated by Au nanobumps. The results imply us that arranging Au nanobumps can construct the scatting imaging of plasmonic projection. In this letter, we experimentally investigate the scattering behavior of surface plasmonic waves generated by the various plasmonic structures, which is composed of Au nanobumps on an Au thin film. We would like to find out the far-field focusing properties of the plasmonic curve structure and control it via changing the geometry of curve structure. The

Plasmonics in Biology and Medicine XI, edited by Tuan Vo-Dinh, Joseph R. Lakowicz, Proc. of SPIE
Vol. 8957, 89570V · © 2014 SPIE · CCC code: 1605-7422/14/$18 · doi: 10.1117/12.2038220

focusing and diverging plasmonic nanostructures are fabricated on the same surface of Au film to be imaged and studied simultaneously. Moreover, we propose a simply method to design the structures that will exhibit plasmonic projection of imaging. It demonstrates the utility of three dimensional light projection of specific light pattern by manipulating scattering light from designed Au nanobumps arrays.

2. EXPERIMENTAL

2.1 Ultrashort-pulse laser fabrication system

Subwavelength artificial structures are fabricated by ultrashort-pulse laser fabrication system, which was used in past experiments.[17-18] A femto-second laser beam with the center wavelength 800 nm, in which the pulse duration is 140 fs and repetition rate 80 MHz, radiated from a Ti:sapphire laser system (Coherent Inc.) is used. The high-numerical aperture oil-immersion objective lens (Zeiss Plan-Apochromat, 100×, 1.4 NA, 0.17 mm working distance) is employed to tightly focus the circular polarized laser beam. The gold thin film was sputtered on a glass substrate, and its thickness is 30 nm. By laser direct writing (LDW) technique, the surface of gold film will be fast modified by focused-laser illumination. Controlling the proper power and exposure time of laser, the laser energy will be absorbed and the gold thin film can be rose up as a subwavelength nanobump structure by way of the laser-induced melting.[19] For investigation the interaction of nanobumps, the nanometer precision stage (Mad City Lab. Inc., Nano-LP200) is used to control interspacing of adjacent nanobumps and arrange it as a designed plasmonic structure. The surface morphology of the fabricated structure is characterized by an atomic force microscope (AFM) (Asylum Research, MFP-3D).[20] All nanobumps in each structure shown in this paper are fabricated in laser power 240 mW and exposure time 30 ms, and the processes were carried out in air at room temperature.

2.2 Total internal reflection microscope system

Total internal reflection microscope (TIRM) system is introduced for the investigation of the light manipulation by the fabricated nanobumps.[21] In order to excite the surface plasmon wave, a fiber illuminator coupling 532-nm Nd:YAG laser as a excitation source is built up to control incidence angle, which satisfy the momentum conversion between the surface plasmon wave and incident light. In this setup for measurements, the oil-immersion objective (Olympus, Plan-Apo Oil TIRFM, 60×, N.A. 1.45) is used not only for launching surface plasmon wave, but for collecting the scattering light. The reflected laser beam will be blocked by the stop, and dark field image of scattering light can be captured by a CCD camera (Hamamatsu Co., ORCA-ER). For observation the propagation behavior of scattering light, we adjust the focal plane of the objective along the z-axis to construct the trajectories of scattered light in 3-D. The polarization of incident beam is set by the polarizer. All experiments are carried out by illuminating TM-polarized laser beam with incident angle of 45° for launching surface plasmon wave.

3. RESULTS AND DISCUSSION

The topography and TIRM optical images of the curve structures with different radii of curvature (RCs) are shown in Fig. 1. Figure 1a shows the AFM image of the structures fabricated by femto-second laser on a 30 nm Au thin film. It is arranged by 21 nanobumps with interspacing 450 nm with different RCs. The average height and the diameter of the base of each nanobump in every structure are 19.7 nm and 303.3 nm, respectively. The propagation direction of surface plasmon wave is along y direction. Impinging on the structures, the incoming surface plasmonic wave is scattered and imaged by CCD camera. In Figs. 1b, we show TIRM images of the curve structures, which are at different locations of focal planes z, and the images are captured when focusing patterns are observed. Both concave (left column) and convex (right column) structures with various RCs, the focusing patterns composed of a focusing spot with two optical arms are observed. In concave structure with larger RC, the focusing pattern is observed at deeper focal plane away from Au surface. On the contrary, in convex structures with larger RC, it is observed at higher focal plane. For close look at the focusing patterns, it can be seen that the smaller bright spot with two short and inward optical arms in the both structures with r = 2.9 μm. Along with increasing the RC, the length of central spots and separation of two optical arms are gradually longer and larger, respectively. It is apparent to find out that there is the non-neglectable deviation in geometrical shape of focusing patterns under various RCs. In addition, the various RCs of curve structures also bring about the difference in z location where we observes the focusing pattern.

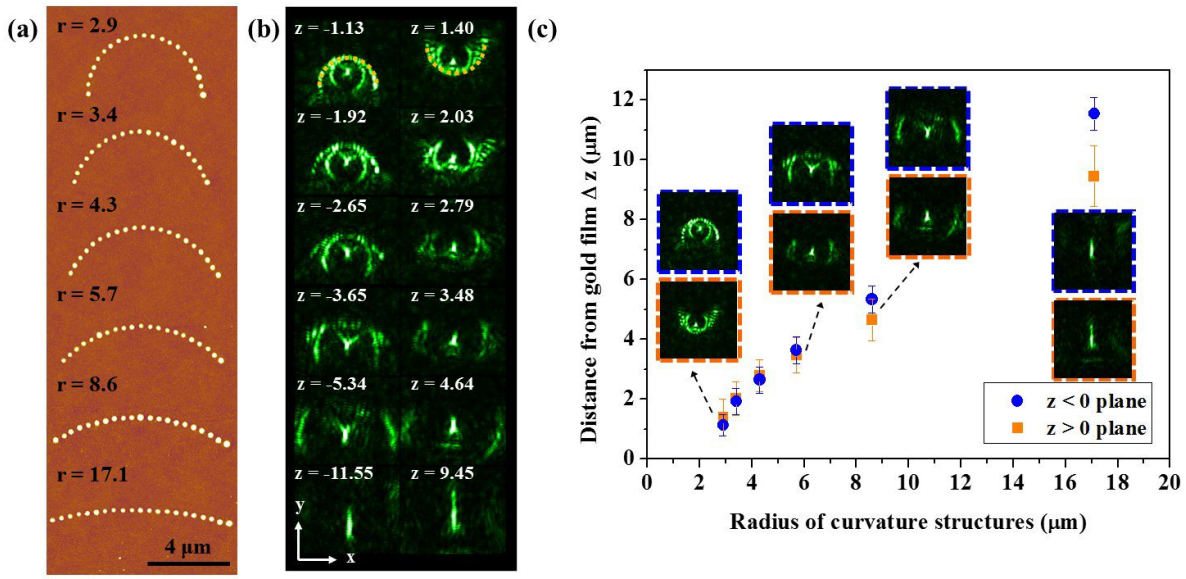

Figure 1.The curve structures with different radii of curvature (RCs). (a) The AFM images of the radii of curvature structure, ranged from r = 2.9 to 17.1 μm. (b) The TIRM optical images of the radii of curvature structure. The left and right columns are the optical images of the concave and convex structure, respectively. (c) The projecting distance from gold film Δz as a function of radii of curvature structures.

For quantifying the relation between z location of focusing pattern and curvature of structure, the plot of the location as a function of structure RC is shown in Fig 1(c). It can be seen that it is positive proportion for both regions of below Au surface $z < 0$ and above Au surface $z > 0$. The inset shows the corresponding focusing patterns. It is worthwhile to note that the variation of distances is up to 10 μm with larger RC. If we desire where the focusing pattern is located, it can performed by selecting the proper RC. However, in case of large RC, the focusing pattern will be seriously distorted, such as the stretched focusing spot in the structure with r = 17.1 μm. Although there is distortion in large RC, it is still controllable for the RC lower than 10 μm.

Figure 2 are the topography and TIRM optical images of the quarter circular structures with different number of nanobumps. Fixing the curvature (r = 5.7 um) of the structures, 11 to 31 nanobumps are choose to set in order for the quarter circle. Therefore, the interspacing of two adjacent nanobumps is from 900 to 300 nm for 11 to 31 nanobumps, respectively. The AFM images of quarter circular structures with the interspacing 300 to 900 nm are shown in Fig. 3a. The average height and diameter of base of nanobumps in every structure, except for the case of interspacing 300 nm, are 16.7 and 296.3 nm, respectively. For the case of smaller interspacing 300 nm, the average height and diameter of base of nanobump are relative small as 8.9 and 193.1 nm, respectively. The reason of the discrepancy may be considered that the overlapping area effect of femto second laser illumination in sequent laser shots. Because of smaller interspacing of adjacent nanobumps, there is significance squeezing restraint when a nanobump rises beside others.

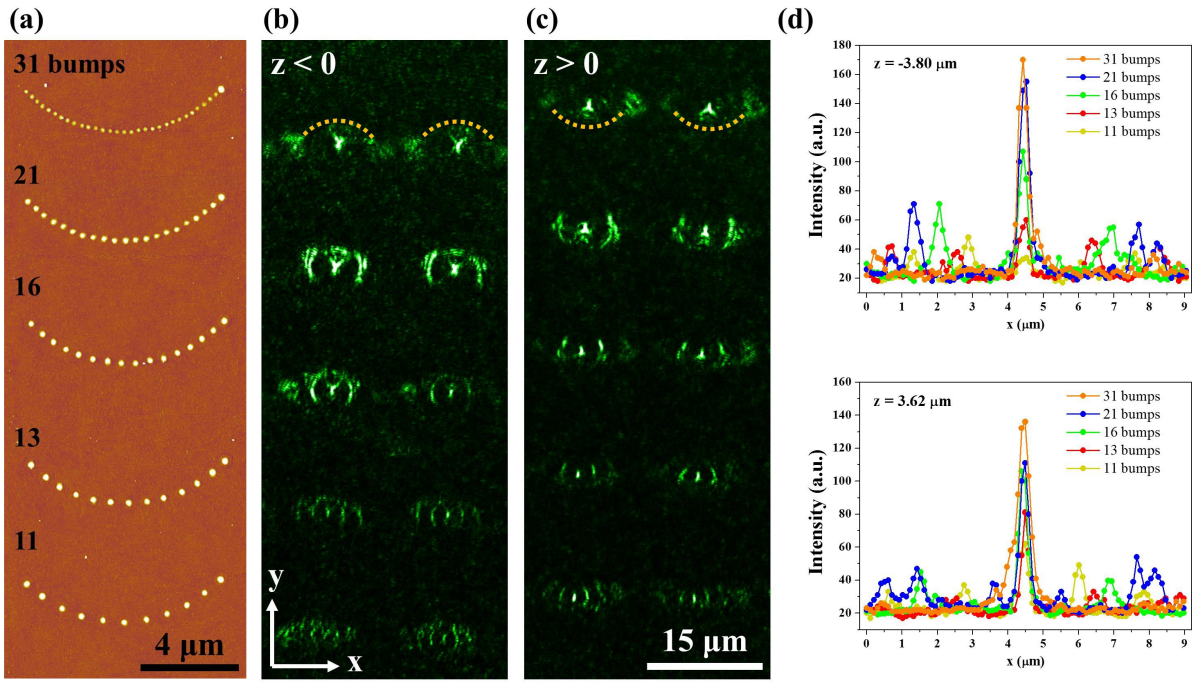

Figure 2. The quarter circular structures with different number of nanobumps. (a) The AFM images of fabricated quarter circular structures with different number of nanobumps. (b) (c) The TIRM optical images of the quarter circular structures with different number nanobumps. The left (b) and right (c) columns are the optical images of the concave and convex structure, respectively. The optical images are observed at $z < 0$ for concave case and $z > 0$ for convex case. (d) The intensity distribution along x direction as a function of concave and convex structures.

The TIRM images of the curve structures with different interspacing are shown in Fig. 2(b)-(c). As previous discussion, its show that the focusing patterns are observed in convex and concave structures, respectively. With different interspacing in curve structures, it can be observed from Fig. 2(b) that there are a bright spot and multiple optical arms in the concave structure with larger interspacing. For concave structure with smaller interspacing, the amount of optical arms can even reduce almost, such as the concave structure with 300-nm interspacing in the top of Fig 2(b). And then the observation plane is set above Au surface, $z = -3.80$ μm, it also can be seen the bright spot and multiple optical arms in concaves with larger interspacing, as shown in Fig. 2 (c).

Figure 2 (d) shows the intensity profile of focusing pattern for the concave and convex with different interspacing. The cross-section of intensity profiles are transverse across focusing patterns. In the both cases of concave and convex, Fig. 2 (d) clearly shows intensity peaks of cross-section on the five structures with different interspacing. The central peak comes from the bright spot, and others are from optical arms. It is clearly shows the number of optical arms is dominated by the interspacing of adjacent nanobumps. The intensity of central peak is increased with smaller interspacing. Because of the smaller interspacing corresponding to more nanobumps, it is intuition for considering the more nanobumps contribute more intensity of scattering light. It means that each nanobump in curve structure can be regarded as an obstacle for surface plasmon wave, and each one contribute the far-field scattering radiation with a small intensity.

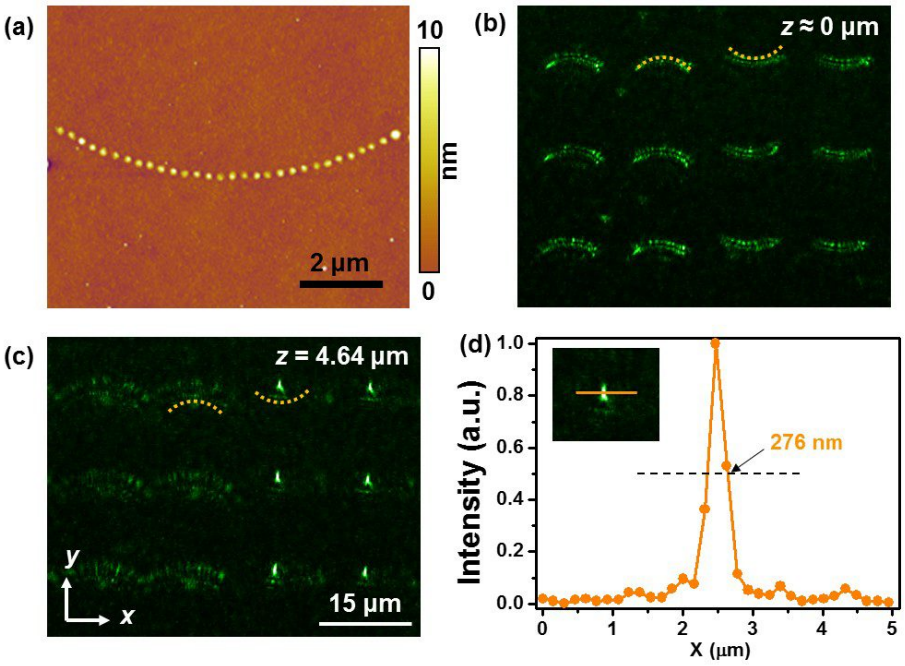

Figure 3. The designed curved structure with r = 8.6 μm and interspacing of 300 nm. (a) The AFM image of the designed curved structure. (b) The TIRM image observed in the observation plane z ~ 0. The bright scattering of concave and convex are shown. (c) The TIRM image in the observation plane z = 4.64 μm. The focusing spot and diverging fringe of convex and concave are observed respectively.

According previous results, the scattering light can be constructed by geometrical parameters of curve structure. If we precise choose the particular curve structure with appropriate curvature and numbers of nanobumps, we can construct a purely single focusing spot. It is necessary for achieving projection imaging. Therefore, the radius of curvature r = 8.6 μm is chosen for light projection away from Au surface. And, the 300-nm interspacing is chosen for generating the single focusing spot. The AFM and TIRM images of the designed curve structure are shown in Fig. 3. In Fig 3 (c), it show that there are purely single focusing spots not only in the convex at z = 4.64 μm and diverging fringe in the concave. In Fig. 3 (b), it shows the bright scattering of nanobumps at Au surface. The intensity profile of the focusing spot is shown in Fig. 3 (d). The FWHM of the intensity profile of focusing spot is around 276 nm, and it is about half of the excitation wavelength of 532 nm. The upper-left inset shows the transversal direction of intensity profile in TIRM image.

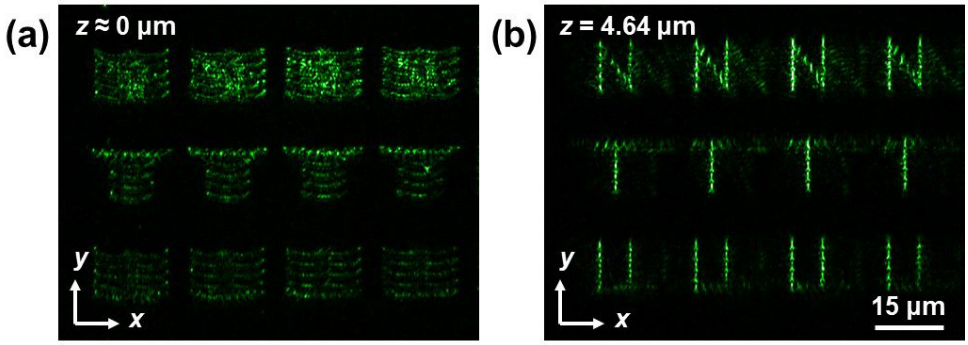

Figure 4. The TIRM images of designed structure composed of the curved structure. (a) The irregular light pattern in the observation plane z ~ 0 μm. (b) The clearly optical pattern "NTU" in the designed observation plane, z = 4.64 μm.

On the purpose of light projection, we demonstrate a simple way to present the light projection image by designed structure. It is intuition to construct the image by pixels. Therefore, the curved structure with proper geometric parameters that demonstrated the single focusing spot in Fig. 3 is adopted as the building block for one pixel in

optical image. This particular curved structure has the ability to focusing scatter light from SPP wave at specific attitude by choosing the proper radius of curvature. Figure 4 shows the TIRM images of designed structure. In Fig 4 (a), the bright scattering of nanobumps from the designed structures are clearly observed. It shows the irregular light pattern at this observation plane, $z \sim 0$ μm. At observation plane $z = 4.64$, as shown in Fig. 4 (b), the TIRM image clearly shows the "NTU" which is projected by designed structure in free space. The concept of light projection by controlling the far-field scattering light is practical.

4. CONCLUSION

In summary, we have fabricated the various plasmonics structures composed of nanobumps on Au thin film by using femto-second laser direct writing method, and shown light manipulation and projection realized by surface plasmon wave scattering. Results clearly demonstrate that the location of focusing pattern from concave and convex structures can be modulated by adjusting the RCs of both, and also the interspacing of adjacent nanobumps in curve structures dominates the numbers of optical arms in focusing pattern. It is interesting to note that the optical results of plasmonic curve structures shown here are based on the same principle: interference of scattering light from surface plasmons wave impinging nanobumps. By precise choosing the curve structure with well-defined RC and interspacing of nanobumps and arranging it with a simply way, we successfully demonstrate the light projection at desire location. Therefore, the utility of three-dimensional light projection can be achieved as long as the arrangements of laser-made Au nanobumps are precisely designed. We believe our research can be further generalized and expanded to more complicated structures that can control and manipulate light in various ways, and provide great potential for versatile nanophotonics applications, such as three dimensional multiple light imaging, miniaturized optical data storage pick-up head focusing, and 3-D integrated photonic circuits.

REFERENCES

[1] Barnes, W. L.; Dereux, A.; Ebbesen, T. W., "Surface plasmon subwavelength optics," *Nature* 424, 824-830 (**2003**).

[2] Wei, H.; Li, Z.; Tian, X.; Wang, Z.; Cong, F.; Liu, N.; Zhang, S.; Nordlander, P.; Halas, N. J.; Xu, H., "Quantum Dot-Based Local Field Imaging Reveals Plasmon-Based Interferometric Logic in Silver Nanowire Networks," *Nano Letters* 11, 471-475 (**2011)**

[3] Drezet, A.; Koller, D.; Hohenau, A.; Leitner, A.; Aussenegg, F. R.; Krenn, J. R., ""Plasmonic crystal demultiplexer and multiports," *Nano Letters* 7, 1697-1700 (**2007)**

[4] Atwater, H. A.; Polman, A., "" *Nature Materials* 9, 205-213 (**2010)**.

[5] Oulton, R. F.; Sorger, V. J.; Zentgraf, T.; Ma, R. M.; Gladden, C.; Dai, L.; Bartal, G.; Zhang, X., "Plasmon lasers at deep subwavelength scale," *Nature* 461, 629-632 (**2009)**.

[6] Fang, Y.; Wei, H.; Hao, F.; Nordlander, P.; Xu, H., "Remote-Excitation Surface-Enhanced Raman Scattering Using Propagating Ag Nanowire Plasmons," *Nano Letters* 9, 2049-2053 (**2009)**.

[7] Peng, T. C.; Lin, W. C.; Chen, C. W.; Tsai, D. P.; Chiang, H. P., "Enhanced Sensitivity of Surface Plasmon Resonance Phase-Interrogation Biosensor by Using Silver Nanoparticles," *Plasmonics* 6, 29-34 (**2011)**.

[8] Kawata, S.; Inouye, Y.; Verma, P., ""Plasmonics for near-field nano-imaging and superlensing," *Nature Photonics* 3, 388-394 (**2009)**

[9] Wood, B.; Pendry, J. B.; Tsai, D. P., "Directed subwavelength imaging using a layered metal-dielectric system," *Physical Review B* 74, (11) (**2006)**.

[10] Bardhan, R.; Lal, S.; Joshi, A.; Halas, N. J., ""Theranostic Nanoshells: From Probe Design to Imaging and Treatment of Cancer," *Accounts of Chemical Research* 44, 936-946 (**2011)**.

[11] Yin, L. L.; Vlasko-Vlasov, V. K.; Pearson, J.; Hiller, J. M.; Hua, J.; Welp, U.; Brown, D. E.; Kimball, C. W., "Subwavelength focusing and guiding of surface plasmons," *Nano Letters* 5, 1399-1402 (**2005)**.

[12] Teperik, T. V.; Archambault, A.; Marquier, F.; Greffet, J. J., "Huygens-Fresnel principle for surface plasmons," *Optics Express* 17, 17483-17490 (**2009)**.

[13] Ditlbacher, H.; Krenn, J. R.; Schider, G.; Leitner, A.; Aussenegg, F. R., "Two-dimensional optics with surface plasmon polaritons," *Applied Physics Letters* 81, 1762-1764 (**2002)**.

[14] Zayats, A. V.; Smolyaninov, II; Maradudin, A. A., "Nano-optics of surface plasmon polaritons," *Physics Reports-Review Section of Physics Letters* 408, 131-314 (**2005)**.
[15] Lester, M.; Skigin, D. C., ""An optical nanoantenna made of plasmonic chain resonators," *Journal of Optics* 13, (**2011)**.
[16] Kumar, M. S.; Piao, X.; Koo, S.; Yu, S.; Park, N., "Out of plane mode conversion and manipulation of Surface Plasmon Polariton Waves," *Optics Express* 18, 8800-8805 (**2010)**.
[17] Chang, C. M.; Chu, C. H.; Tseng, M. L.; Huang, Y. –W.; Huang, H. W.; Chen, B. H.; Huang, D. –W.; Tsai, D. P., "Light Manipulation by Gold Nanobumps," *Plasmonics* 7, 563-569 (**2012)**.
[18] Tseng, M. L.; Chen, B. H.; Chu, C. H.; Chang, C. M.; Lin, W. C.; Chu, N.-N.; Mansuripur, M.; Liu, A. Q.; Tsai, D. P., "Fabrication of phase-change chalcogenide Ge2Sb2Te5 patterns by laser-induced forward transfer," *Optics Express* 19, 16975-16984 (**2011)**.
[19] Meshcheryakov, Y. P.; Bulgakova, N. M., "Thermoelastic modeling of microbump and nanojet formation on nanosize gold films under femtosecond laser irradiation," *Applied Physics a-Materials Science & Processing* 82, 363-368 (**2006)**.
[20] Chang, C. M.; Chu, C. H.; Tseng, M. L.; Chiang, H. P.; Mansuripur, M.; Tsai, D. P., "Local electrical characterization of laser-recorded phase-change marks on amorphous Ge2Sb2Te5 thin films," *Optics Express* 19, 9492-9504 (**2011)**.
[21] Huang, H. J.; Yu, C. P.; Chang, H. C.; Chiu, K. P.; Chen, H. M.; Liu, R. S.; Tsai, D. P., "Plasmonic optical properties of a single gold nano-rod," *Optics Express* 15, 7132-7139 (**2007)**.
[22] Chang, C. M.; Tseng, M. L.; Cheng, B. H.; Chu, C. H.; Ho, Y. Z.; Huang, H. W.; Lan, Y.-C.; Huang, D.-W.; Liu, A. Q.; Tsai, D. P., "Three-dimensional plasmonic micro projector for light manipulation," Advanced Materials 25, 1118-1123 (2013)